



Stockholm
University

Bachelor Thesis

Degree Project in
Marine Geology 15 hp

The late Holocene ^{14}C reservoir age in the Chukchi Sea as inferred from tephra in marine sediments

Aron Varhelyi



Stockholm 2016

Department of Geological Sciences
Stockholm University
SE-106 91 Stockholm

This is my bachelor thesis project-
It is the product of laboratory work,
reading and writing that was done during
ten weeks in the spring of 2016.

Table of Contents

Abstract	4
Introduction.....	5
Methods	7
Field site and sampling.....	7
Tephra.....	8
Electron Probe Micro-Analysis (EPMA)	8
Grain size analysis.....	8
Results	9
Tephra quantification, 5cm samples	9
Tephra quantification, 1cm samples	9
Tephra geochemistry.....	9
Grain size analysis.....	11
Discussion	13
Comments on methods	13
Identification	14
Reworking.....	14
Aniakchak tephra age	15
Placing the isochron	16
Conclusions.....	18
Acknowledgements	19
References.....	19

Abstract

Volcanic ash, or tephra, blankets the local and regional landscape following a volcanic eruption.

If this ash layer is preserved and identified, it can act as a time synchronous marker bed (isochron) for correlation between marine, terrestrial, glacial and lacustrine deposits. This can be a powerful tool when attempting to determine the true age of a marine sample (e.g. clam or mollusk), affected by the marine reservoir effect (MRE). The MRE causes dated radiocarbon to appear the age that carbon was last in equilibrium with the atmosphere rather than the time that a dated material was deposited.

The offset (in years) caused by the MRE is referred to as ΔR . Presented in this study is new data on the lowermost part of SWERUS-L2-2-PC1 (2PC), a marine sedimentary core retrieved from the Chukchi shelf north of Siberia. By using quantification of rhyolitic tephra to locate tephra-rich layers for further study, results show a thick layer that is interpreted to have originated from the caldera-forming eruption of Aniakchak (Aniakchak II). The geochemical identification of the tephra was done using electron probe micro-analysis. A grain size analysis was also conducted to learn more about the sedimentology of 2PC and the possible proxies that can be used when trying to determine where to place the isochron.

The isochron was finally placed with the help of relevant literature and the results from this study. That position shifted the previous age model of 2PC at a position to yield a ΔR of 482 years for the Chukchi Sea during this time period.

Introduction

Volcanic eruptions produce large amounts of ash or *tephra*. Tephra consist of lithics, mineral fragments, pumice and tiny glass shards of quenched magma, which are released into the atmosphere. These shards blanket the landscape, forming deposits of varying thickness; from layers so thin that cannot be seen by the naked eye (cryptotephra), to deposits that are several meters thick. Thicknesses of deposits are controlled by the magnitude of an eruption, distance to the volcano, transport mechanisms and post-deposition processes whereas the range of tephra fallout is limited by the magnitude of eruption, as well as prevailing winds. Since the fallout is close to instantaneous, from hours to months (Lowe, 2011), the tephra beds can be used as *isochrons* if found in a sedimentary column. This can greatly assist in sediment age correlation which is why tephrochronology is a field of research. By using the law of superposition, an identified tephra layer that is found can be used as a time synchronous marker, which ties sedimentary records together. As a relative time marker tephrochronology is very useful indicating leads and lags in the climate system. However, it is as an absolute age marker that tephra layers are most useful - when given an approximate age. That ties all tephra layers resulting from the same eruption to that age.

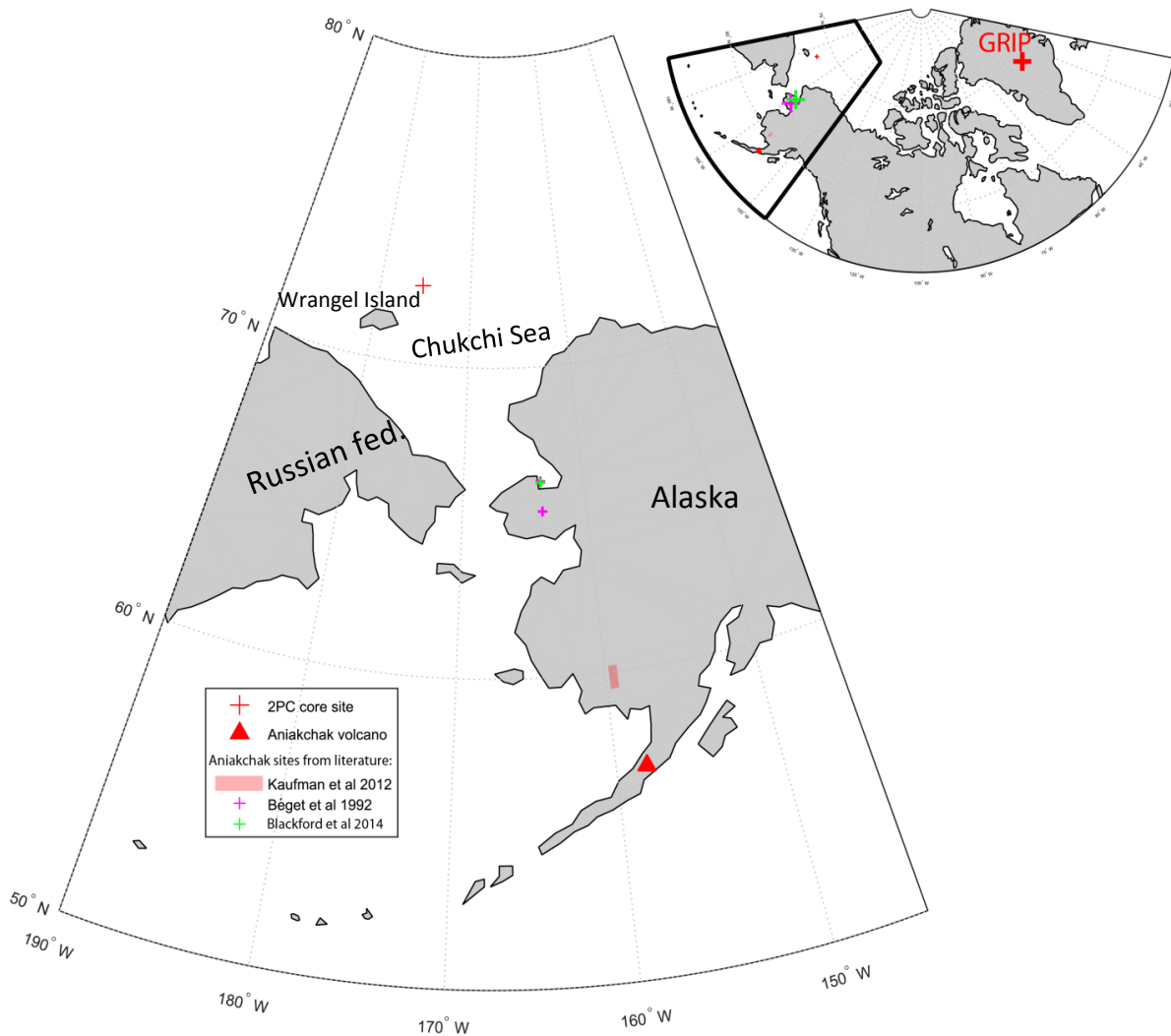


Figure 1. Map including the core site for 2PC (this study) along with study sites from selected previous works.

A successful correlation of tephra, or cryptotephra, depends on: (i) a geochemical identification of the tephra, (ii) investigation of a sedimentary deposit that hasn't been reworked by post-depositional processes, (iii) radiocarbon dating of adjacent layers and (iv), for the marine environment, knowing the reservoir age of dated radiocarbon surrounding the tephra bed (Lowe, 2011).

A marine setting could complicate above points (ii) and (iv). Bioturbation by burrowers and other animals could transport sediment up and down a column thus diffusing a signal (Clough, et al. 1997; Griggs, et al. 2015). Walker (2005) describes the problem with the reservoir age of marine radiocarbon; how many years have passed between uptake of atmospheric radiocarbon and deposition of dated material?

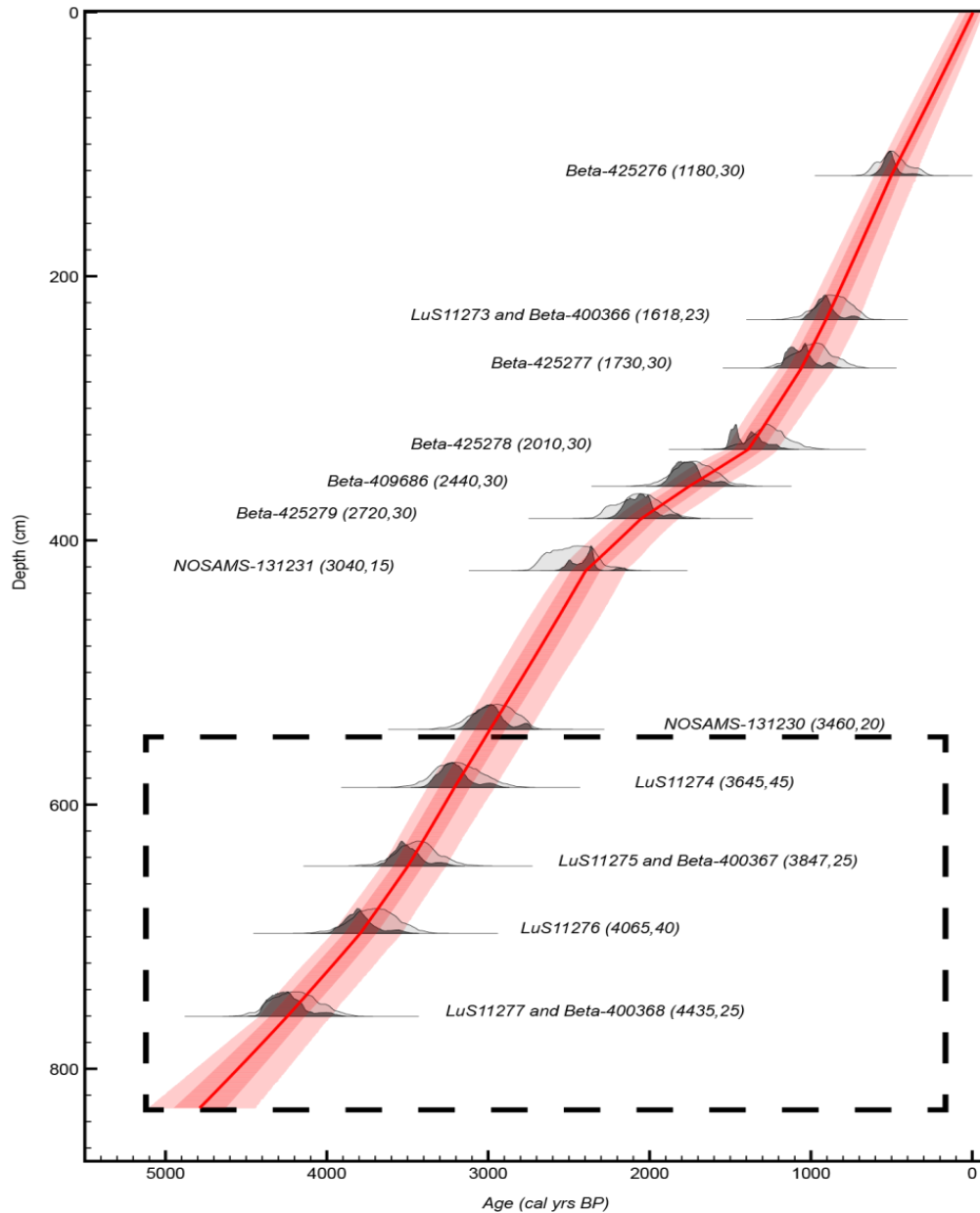


Figure 2. Chronology of SWERUS-L2-2-PC1 (2PC) based on 15 radiocarbon samples. Chronology was constructed by Christof Pearce, Department of Geology, Stockholm University. Fading red indicate the calculated uncertainty. Dotted line demarcates focus for this study.

This effect is sometimes referred to as the Marine Reservoir Effect (MRE). Resulting from the MRE is an offset in radiocarbon age between a terrestrial and marine setting. This marine reservoir age is called R and is on average 400 years. There is however significant geographic (and temporal) variation in this reservoir age which expressed as ΔR , the deviation of this common reservoir age R .

This ΔR is unique for each marine setting and can vary from negative (almost atmospheric) to more than 1000 years in places with very old carbon input. Other factors that could influence the strength of a tephra signal is sedimentary drift caused by currents, and delayed input of tephra by terrestrial runoff and ice berg transport (Austin, et al., 1995).

The chronology of the marine sediment core SWERUS-L2-2-PC1 (hereafter 2PC) (Figure 1) is based on 15 radiocarbon dates which indicate an age span from ca. 5000 cal. yrs. BP to present day (Figure 2). Despite the high density of radiocarbon dates, sample age uncertainties are probably still in the order of centuries, due to the unknown marine reservoir age of the region. Currently, a reservoir age of 300 ± 100 yrs. is being used.

The aim of this bachelor thesis project is to improve this by obtaining an absolute age marker, which allows correlation to well-dated terrestrial or ice-core sites with much lower age uncertainties.

A pilot study of samples from 2PC has indicated high concentrations of volcanic ash particles around the expected age of the Alaskan so called Aniakchak tephra which has an age of 3591 ± 3 years BP based on its identification in the GRIP ice core (Abbott and Davies, 2012).

The Plinian Aniakchak caldera forming eruption (hereafter Aniakchak II) with a volcanic explosivity index (VEI) of 6, was one of the largest during the Holocene, ejecting over 50 km^3 of volcanoclastic material in a probable 25km high column (Blackford, et al. 2014; Begét, et al., 1992).

The proximal and regional tephra deposits created thereof have previously been studied by e.g. Kaufman, et al. (2012), Begét, et al. (1992), Riehle, et al. (1987) and Blackford, et al. (2014). However, supposed tephra deposits of the same origin have also been found in the GRIP (Greenland Ice Core Project) ice core (Abbott and Davies, 2012; Vinther, et al. 2006; Hammer, et al. 2003).

The origin of the GRIP tephra layer has been in dispute: Hammer, et al. (2003) first identified the layer and assigned it to the Minoan Thera eruption (Greece). Pearce, et al. (2004) reevaluated the tephra geochemistry, finding the offset in major elements too high, and suggested Aniakchak II as source. Vinther, et al. (2006) found an acid peak/tephra layer discrepancy which lead them to support Thera. However, Abbott and Davies (2012) support the Alaskan Aniakchak II eruption as source on the basis that no tephra shards related to the Thera eruption has been found in any of the Greenland ice cores, making Thera an unlikely source.

Methods

Field site and sampling

The core on which all sampling and data collection was done for this thesis was the 2PC marine sediment core. It was retrieved in 2014 during the SWERUS expedition east of Wrangel Island in the Chukchi Sea (72.516580 N , -175.319605 W) using a piston corer on the ice breaker R/V Oden. The water depth was 72 meters and the core totaled 8.21 meters. The core was split in eight sections measuring ca. 1.5 m each.

Sedimentation rates at the coring site are high; in the order of 6cm/yr. for the entirety of the core and 7cm/yr. for the investigated sections.

The aim of this project was to find the Aniakchak II eruption and the sampling therefore took a targeted approach. The lowest 2.5m of the core were analyzed to make sure that the 3600 cal. yrs. BP volcanic event was captured. This study focuses on core sections 5 and 6 which represent 548.5-821.5 cm dbfs (depth beneath sea floor)(Figure 2) and 3014.9-4719.3 years BP according to the original chronology shown in Figure 2. Four sets of samples have been used in this study:

1. Test sampling for a pilot study by Stefan Wastegård, Department of Physical Geography, Stockholm University. These twenty pilot samples span from 40 cm depth in section 5 to 15 cm depth in section 6. They were quickly studied to scan for possible tephra shards before this project started and named TP (Tephra Pilot).
2. 5cm long samples of ca. 1g dry weight were extracted throughout both sections to create a rough view of tephra concentrations. Samples were taken without gaps so as not to miss any layers.
3. 1cm samples of c 1g were extracted at depths consistent with the highest tephra concentrations surrounding what was initially believed to be the Aniakchak II eruption. This was done to increase resolution and to pinpoint the exact depth of the maximum.
4. Grain size analysis with 1 cm spacing over 1m depth range, including both minimum and maximum tephra concentrations.

Tephra

Tephra quantification was done on sample sets 2 and 3. The tephra was isolated through sieving using a 25 μ m nylon fabric thus keeping the >25 μ m particles. These particles were then subjected to heavy liquid separation where only particle densities of 2.3-2.5 g/cm³ were kept, which is consistent with rhyolitic tephra. This method is described in detail by Turney (1998).

To the remaining particles, lycopodium spores of a known amount were added. From that, a ratio of tephra/spores could be used to calculate tephra particles per gram after mounting the mix of tephra and spores on microscope slides. When counting, tephra particles of <40 μ m were rejected under x20 microscopy. Tephra is identified by its glassy appearance; sharp edges, random fractures, transparent, and isotopic character. Counted tephra particles are in the size of 40-340 μ m.

Electron Probe Micro-Analysis (EPMA)

Microprobe analysis using the JEOL JXA-8530F Hyperprobe at Uppsala University was done on selected samples from set 1: TP 7, TP 10 and TP 20 which represents core depths of 624cm, 639cm and 687cm.

These samples all showed to contain tephra during the pilot study, which is the reason why they were chosen. Data was obtained with a 15kV, 4 nA beam current with a beam diameter of 10 μ m.

Ten tephra shards per sample with a >94% total were chosen, in a second step, to analyze for major elements expressed in oxides (Na₂O, SiO₂, Al₂O₃, MgO, K₂O, CaO, TiO₂, FeO and MnO). The results are presented together with a mean normalized to 100% and standard deviations.

Grain size analysis

Based on the quantification of tephra in this study, an interesting part of the two sections was chosen for further grain size analysis. This part contained a peak in tephra concentration, as well as sections where low concentrations could be interpreted as background. The analysis was performed using laser diffraction

measurements by a Mastersizer3000 at the IGV (Institution for Geological Sciences, Stockholm University), with the aim of finding a possible correlation between grain size and tephra concentrations, so that grain size could act as a proxy for tephra or indicate transport of sediment. Samples were taken every cm between 656.5cm-714.5cm in 2PC. From 715.5-746.5, samples were taken every *other* cm. Each wet sample was put in a sodiumhexametaphosphate solution (<10%) and was subjected to ultrasound in order to disaggregate before analysis. Sample sizes were <0.5g of wet sediment.

Results

Tephra quantification, 5cm samples

Tephra was found in all samples in varying amounts. Sizes of the shards range between 25 and 340 μ m but a majority of them are 80-160 μ m. Figure 3 shows one of the more tephra rich samples. The tephra is found to be platy, clear, sometimes fluted, and with occasional crystal inclusions. Figure 4 shows the results of the initial 54 5cm samples. It roughly indicates higher concentrations 550-715cm dbsf. Two peaks are identified at 650-655cm and 665-670cm dbsf. A saw tooth pattern moves along a curve-like increase between 600cm and 715cm dbsf (hereafter *Increase X*).

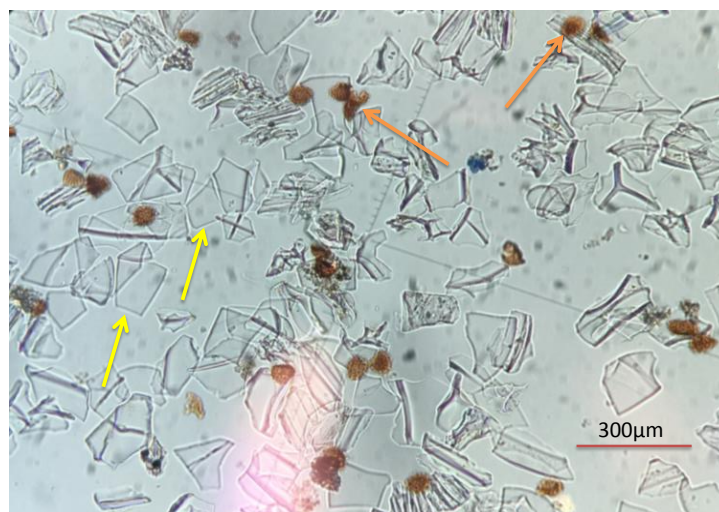


Figure 3. Shards from one of the more tephra-rich samples in 2PC. Yellow arrows point at tephra whereas the orange arrows point to the lycopodium spores that were added for reference. Photo: Aron Varhelyi, May 2016.

Tephra quantification, 1cm samples

These samples were taken to increase resolution and pinpoint the exact depth interval of the identified maxima, possibly the isochron of the Aniakchak II eruption. The results of the 25 samples between 652 and 673cm dbsf shows similar peaks as seen in the 5cm samples, however, tephra counts are overall lower and does not match when averaged.

Tephra geochemistry

The EPMA data presented in Table 1, Table 2 and Figure 6 are based on samples TP7, TP 10 and TP20 (Figure 4 and 5). Ten measurements per TP was included in these tables with the prerequisite of having an oxide total above 94%. The different amounts were normalized to 100% to facilitate comparison with other investigations. Results shows a high degree of clustering; there are no obvious outliers and low standard deviations (Table 1). Data corresponds well with previously studied geochemistries of tephra identified as Aniakchak tephra, as shown in Table 2 and the ternary plot (Figure 6).

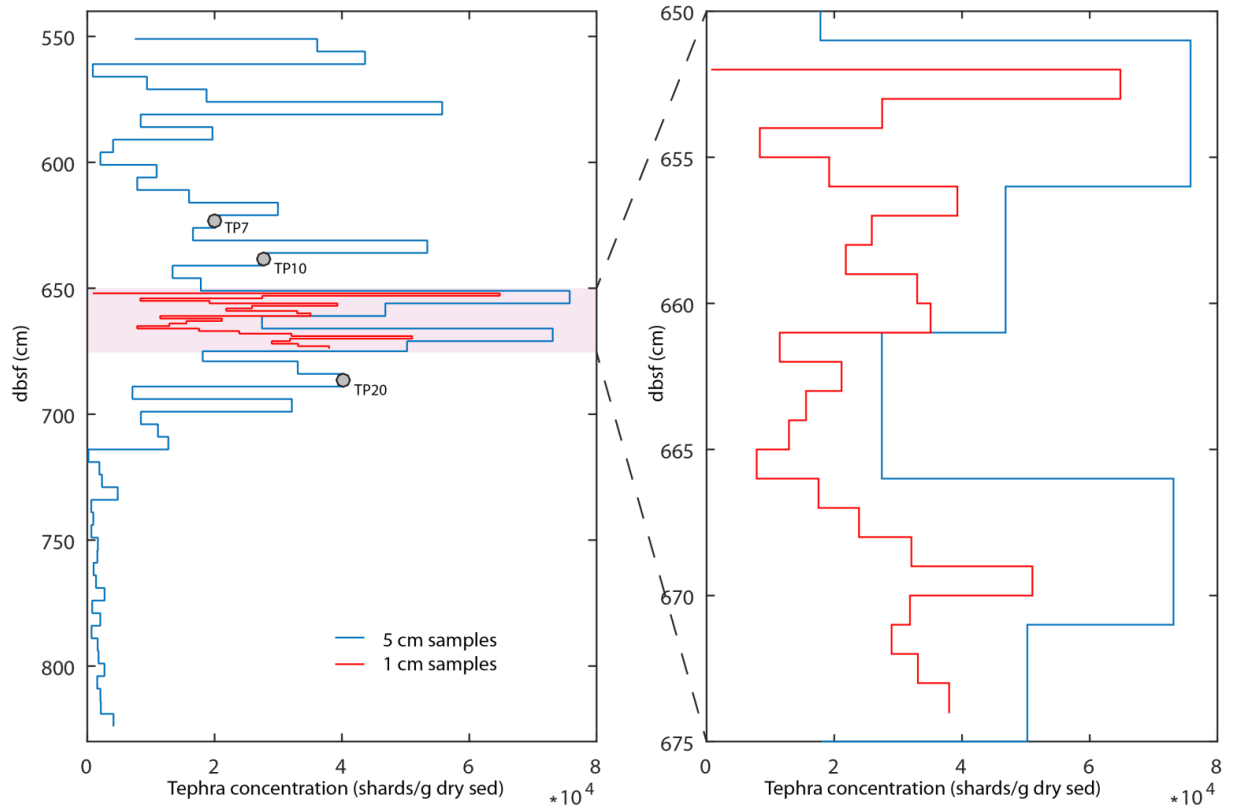


Figure 4. Shards of rhyolitic tephra/g of dry sediment as calculated after heavy liquid separation. Left plot shows total length of investigated core depth with TP (geochemical) samples included. Right plot is a close up of core depth where the 1cm samples were taken. The saw tooth pattern along a curve like tephra increase between 600cm and 715cm dbsf is referred to as *Increase X*.

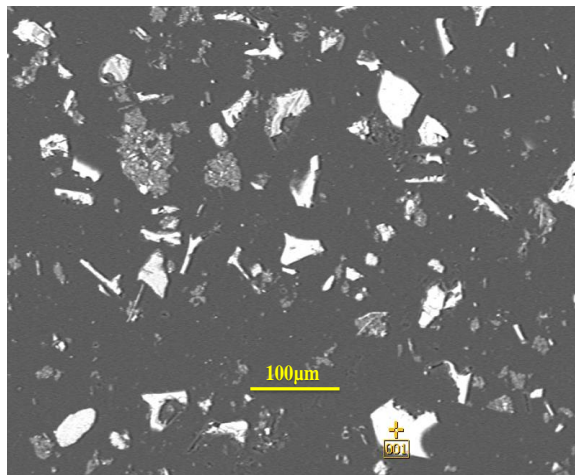


Figure 5. Volcanic tephra from TP20 as seen using the EPMA at Uppsala University. Volcanic tephra are the bright white angular shards

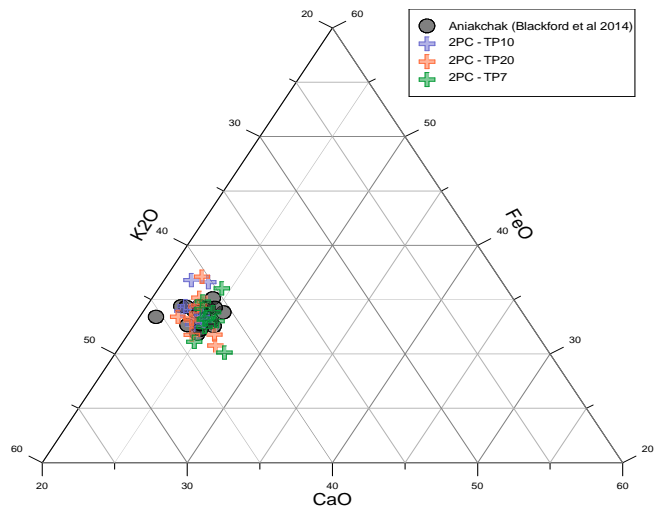


Figure 6. Ternary plot comparing data from this study with previous work on tephra geochemistry identified as Aniakchak tephra. The data has a high degree of overlap and the tephra in this study has therefore been identified as having the caldera forming eruption of Aniakchak (approx.. 3600 BP) as source.

Table 1. Glass geochemical data from 10 samples each for TP7, TP10 and TP20. Data was obtained using the JEOL JXA-8530F Hyperprobe at Uppsala University with a 15kV, 4 nA beam current, and a beam diameter of 10 μ m. The results are presented together with a mean normalized to 100% and standard deviations.

TP7	1	2	3	4	5	6	7	8	9	10	Mean norm.	σ
SiO ₂	72.38	73.13	71.79	72.07	72.08	72.26	72.24	71.72	72.01	71.77	72.15	0.39
TiO ₂	0.46	0.39	0.35	0.4	0.41	0.43	0.44	0.5	0.49	0.52	0.44	0.05
Al ₂ O ₃	14.66	13.84	14.98	15.09	15.24	15.08	14.76	14.92	14.92	14.97	14.85	0.37
FeO	2.3	2	2.61	2.45	2.13	2.25	2.39	2.38	2.31	2.43	2.32	0.16
MnO	0.2	0.19	0.14	0.05	0.07	0.15	0.19	0.1	0.05	0.19	0.13	0.06
MgO	0.47	0.79	0.46	0.71	0.53	0.49	0.5	0.45	0.5	0.53	0.54	0.11
CaO	1.81	1.86	1.8	1.7	1.74	1.76	1.71	1.79	1.75	1.84	1.78	0.05
Na ₂ O	4.82	4.94	4.84	4.6	4.78	4.55	4.75	5.17	4.92	4.61	4.8	0.18
K ₂ O	2.85	2.77	2.82	2.89	2.96	2.9	2.9	2.87	2.91	3.03	2.89	0.07

TP10	1	2	3	4	5	6	7	8	9	10	Mean norm.	σ
SiO ₂	72.46	72.33	72.35	72.35	72.57	72.19	72.23	72.35	71.87	72.32	72.3	0.18
TiO ₂	0.44	0.48	0.39	0.48	0.49	0.47	0.46	0.42	0.46	0.47	0.46	0.03
Al ₂ O ₃	14.75	14.73	14.97	14.82	14.78	14.86	14.74	14.6	15.01	14.81	14.81	0.11
FeO	2.34	2.26	2.52	2.29	2.39	2.27	2.36	2.38	2.66	2.44	2.39	0.12
MnO	0.18	0.1	0.08	0.2	0.14	0.22	0.06	0.13	0.06	0.17	0.13	0.05
MgO	0.59	0.48	0.5	0.51	0.48	0.54	0.54	0.57	0.59	0.53	0.53	0.04
CaO	1.71	1.67	1.51	1.72	1.61	1.68	1.63	1.58	1.69	1.76	1.66	0.07
Na ₂ O	4.51	4.99	4.68	4.69	4.46	4.75	4.9	4.99	4.68	4.28	4.69	0.22
K ₂ O	2.95	2.86	2.82	2.92	3.04	2.98	2.9	2.96	2.91	3.04	2.94	0.07

TP20	1	2	3	4	5	6	7	8	9	10	Mean norm.	σ
SiO ₂	71.58	71.95	72.11	72.59	71.6	71.97	72.09	71.87	71.9	72.26	71.99	0.28
TiO ₂	0.47	0.44	0.42	0.41	0.46	0.37	0.4	0.41	0.45	0.41	0.42	0.03
Al ₂ O ₃	14.84	14.87	14.93	14.65	15.28	15.2	14.91	15.04	15.11	14.8	14.96	0.18
FeO	2.55	2.6	2.12	2.33	2.24	2.19	2.33	2.44	2.31	2.21	2.33	0.15
MnO	0.18	0.15	0.23	0.06	0.18	0.14	0.18	0.11	0.16	0.25	0.16	0.05
MgO	0.43	0.55	0.61	0.51	0.48	0.57	0.53	0.51	0.6	0.54	0.53	0.05
CaO	1.71	1.59	1.85	1.7	1.74	1.5	1.61	1.7	1.67	1.83	1.69	0.1
Na ₂ O	5.2	4.94	4.75	4.73	4.92	5.12	4.99	4.92	4.63	4.73	4.89	0.17
K ₂ O	2.98	2.8	2.91	3.01	3.06	2.85	2.83	2.94	2.97	2.91	2.93	0.08

Table 2. EPMA data averages for TP7, TP10 and TP20 compared with previous studies of Aniakchak tephra. All values normalized to 100%. Standard deviations in parentheses.

Data set	This study, Chukchi Sea			Blackford, et al. (2014), Alaska	Abbott and Davies (2012), Greenland	Riehle, et al. (1987), Alaska		Begét, et al. (1992), Alaska	
	TP7	TP10	TP20		GRIP	7b	8	CE	WL
N	10	10	10	20	174	n.r.	n.r.	16	15
SiO ₂	72.15 (0.39)	72.3 (0.18)	71.99 (0.28)	71.93 (1.27)	70.55 (1.8)	71,25 (0.6)	71,25 (0.6)	71.41 (0.24)	71.36 (0.2)
TiO ₂	0.44 (0.05)	0.46 (0.03)	0.42 (0.03)	0.48 (0.09)	0.89 (0.6)	0,47 (0.06)	0,46 (0.06)	0.45 (0.04)	0.48 (0.03)
Al ₂ O ₃	14.85 (0.37)	14.81 (0.11)	14.96 (0.18)	14.97 (0.2)	14.7 (0.98)	15,21 (0.47)	15,32 (0.48)	14.98 (0.16)	15.05 (0.11)
FeO	2.32 (0.16)	2.39 (0.12)	2.33 (0.15)	2.48 (0.11)	3.34 (1.11)	2,39 (0.09)	2,39 (0.09)	2.64 ^a (0.1)	2.63 ^a (0.14)
MnO	0.13 (0.06)	0.13 (0.05)	0.16 (0.05)	0.36 (0.03)	0.36 (0.41)	0,14 (0.03)	0,15 (0.03)	n.r.	n.r.
MgO	0.54 (0.11)	0.53 (0.04)	0.53 (0.05)	0.53 (0.03)	0.63 (0.49)	0,50 (0.03)	0,52 (0.04)	0.49 (0.04)	0.51 (0.04)
CaO	1.78 (0.05)	1.66 (0.07)	1.69 (0.1)	1.78 (0.11)	2.13 (0.6)	1,74 (0.03)	1,75 (0.04)	1.73 (0.11)	1.75 (0.07)
Na ₂ O	4.8 (0.18)	4.69 (0.22)	4.89 (0.17)	4.59 (0.72)	3.75 (0.88)	5,29 (0.18)	5,23 (0.18)	5.24 (0.17)	5.18 (0.16)
K ₂ O	2.89 (0.07)	2.94 (0.07)	2.93 (0.08)	3.12 (0.1)	3.65 (0.55)	2,97 (0.05)	3,01 (0.05)	2.86 (0.22)	2.87 (0.12)
Total	100	100	100	100	100	100	100	100	100

n.r. = not reported.

^a Begét et al. (1992) report Fe as Fe₂O₃ but is here converted to FeO for comparison.

Grain size analysis

As seen in Figure 8a and 8b, the grain size analysis show that sediments are predominantly (>95%) of fractions <63µm, which is consistent with silt or smaller according to the Udden-Wentworth grain size scale (Boggs, Jr., 2011, p. 46). To be able to see anything of interest through that mud, one has to look closer at small variations in coarser grain size fractions. Figure 8c shows a close up of the distribution of >127µm clasts.

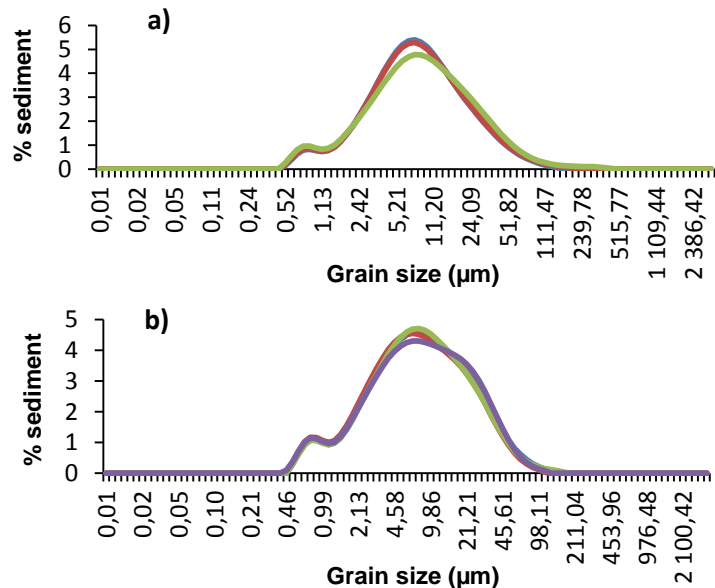


Figure 7. Replicate samples taken at 649.5cm (a) and 677.5cm (b). (a) represents three replicate samples and (b) four.

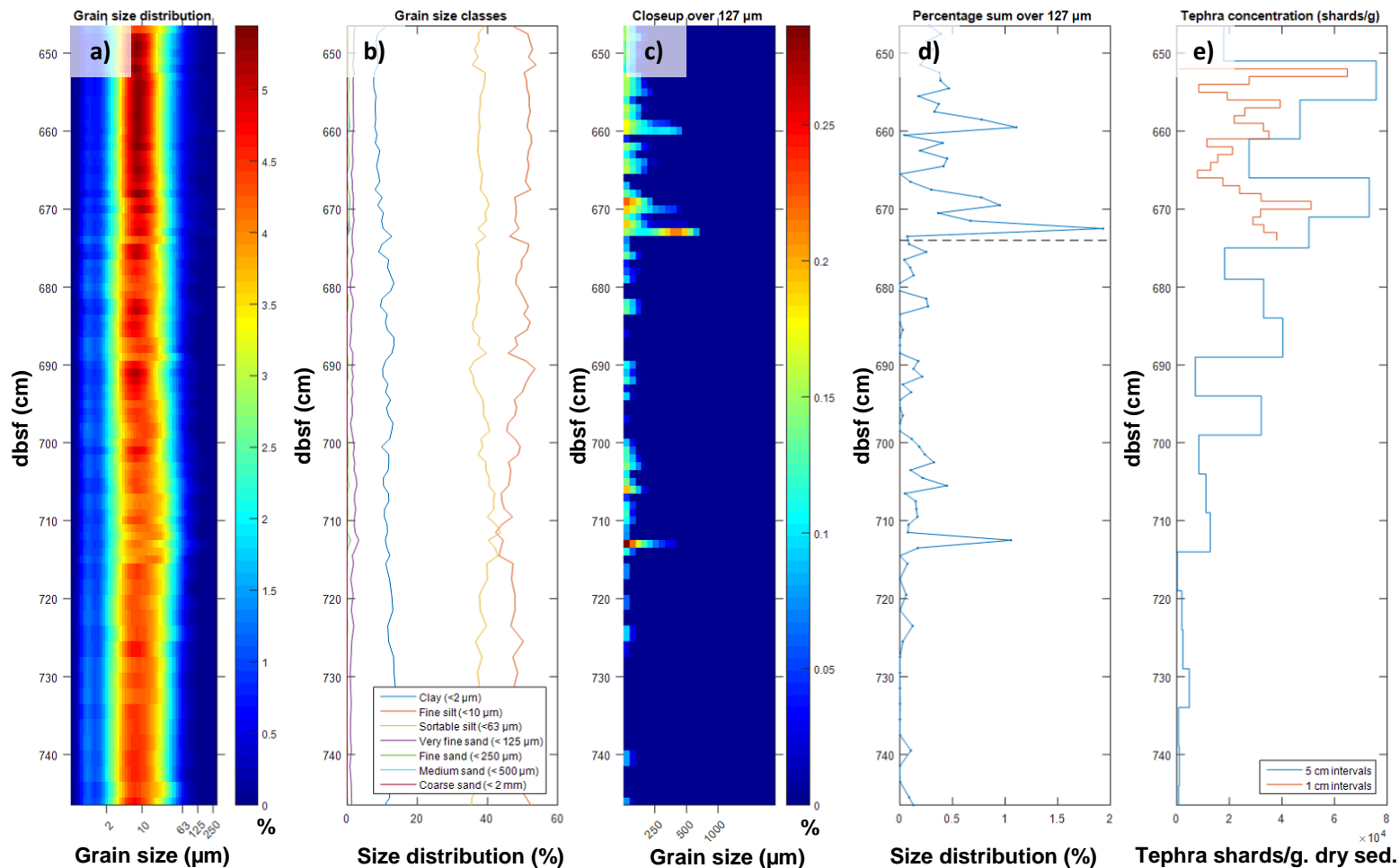


Figure 8. All plots except the (e) one show grain size distributions over the investigated area. The sediment is fairly homogenous and is dominated by silt of various sizes and clay. To find a comparable size fraction, a close up of $>127\mu\text{m}$ clasts was done. This size was chosen due to the output data of the laser diffraction measurements. Note the low percentages of $>127\mu\text{m}$ clasts, but note also how the peaks show possible correlation with peaks in tephra concentrations. Dotted line in (d) illustrates the section break between section 5 and 6.

Discussion

Comments on methods

Although tiny in percentages, the grain size distribution *does* show a correlation with peaks in tephra concentrations (Figures 8d and 8e).

Rather than being a proxy for rhyolitic Aniakchak tephra - a lot of the $>127\mu\text{m}$ clasts are not rhyolitic or tephra, and a great amount of the tephra is $<127\mu\text{m}$ - the peaks in $>127\mu\text{m}$ clasts could indicate an increase in the input of ice rafted detritus (IRD), or other transport mechanism leading to an increase in coarser clast fractions. That could be an important observation when explaining the $>1\text{m}$ spread of *Increase X*, seen in Figure 4, that is likely to have Aniakchak as origin. A possible complication regarding the grain size analysis could be that the small samples ($<0.5\text{g}$) is at risk of being unrepresentative for that depth. Griggs and Davies (2015) have used 3D imagery to visualize how heterogeneous core sediments can be, that is confirmed by the replicate samples taken at 649.5cm and 677.5cm (Figure 7).

Inspired by Kylander, et al. (2011), a comparison was made between XRF data and tephra count data in search for a correlation. This did not yield any convincing results.

The overall lower tephra counts in the 1cm samples are intriguing. The method itself, involves several steps that include handling tiny amounts of particles, which sometimes aren't visible to the naked eye. Sample loss *is* possible. However, sample losses in *all* of the 1cm samples seem unlikely.

There might have been something amiss, with the lycopodium spores, which were added to count a ratio, since the 5cm and 1cm were made using a separate batch of lycopodium tablets. If more spores were added than put into calculation, then counts would drop. Also, the 1cm sample average over 5cm does not match. This could be related to the heterogeneousness of the core sediment or possible unreliability in the method.

Identification

Given that the caldera forming eruption approximately 3.6ka BP was one of the largest during the Holocene (Blackford, et al., 2014; Begét, et al., 1992; Kaufman, et al., 2012), being one of only two tephra layers found in all Alaskan lakes as part the study by Kaufman, et al. (2012), any tephra deposit in this region found at depths corresponding to that age would be suspected to have the Aniakchak II as origin. The data from 2PC presented in this bachelor thesis project shows a saw tooth pattern along a 1.1m curve-like increase (*Increase X*) in tephra between radiocarbon ages of 3288.2 BP and 3889.9 BP (original age model).

The amount of tephra basically flat lines below that curve. Even though tephra *is* found, it is found in such small amounts that it could be considered background.

Taken the MRE into account (which was set to 300 yrs. in the original 2PC chronology), *Increase X* roughly coincides with the Aniakchak II eruption. Furthermore, the visual appearance and size of observed shards in this study is consistent with tephra from previous studies where it has been identified as Aniakchak tephra (Begét, et al., 1992). That is, ca. 40-200µm shards with occasional larger clasts. Visually, they are clear and platy which also is consistent with Begét, et al. (1992) even though Kaufman, et al. (2012) reports bubble-wall and tri-cusped shards.

Finally, the geochemical analysis of TP7, TP10 and TP20 shows good correlation with EPMA data from earlier works (Blackford, et al., 2014; Pearce, et al., 2004; Riehle, et al., 1987; Begét, et al., 1992) as shown in Table 2 and Figure 6 where the geochemical signal has been interpreted as Aniakchak.

One could argue that the positions for the TP samples are less than optimal. However, since all three TP:s are unambiguous in their results and since tephra levels doesn't reach above background level, the 1.1m tephra curve is interpreted as having a single major source.

Because of these correlations, the entirety of *Increase X* (representing c. 3288.2 BP-3889.9 BP) is recognized as the Aniakchak II eruption.

Reworking

The widespread tephra signal over a depth interval of more than 1m raise questions about post-depositional processes, other eruptions and bioturbation – processes that could blur a tephra deposit and complicate the work of locating the isochron. First, above the layer interpreted as Aniakchak are two peaks (Figure 4) between 550cm and 600cm dbsf. These could possibly be correlated to a tephra unit (found as a single deposit) by Kaufman, et al. (2012) who called it the “3.1ka event”.

They showed that that accumulation is geochemically indistinguishable from the Aniakchak deposit.

However, both Kaufman, et al. (2012) and this study show a tephra *low* in between isolating *Increase X*

from the 3.1ka event. Therefore, the 3.1ka event is treated as a different eruption outside the focus of this study.

Second, bioturbation is a process that could transport sediment laterally as well as up and down a sedimentary column. Austin, et al. (1995) used models to determine how far bioturbation of volcanic ash can be transported up or/and down. Their setting was the Hebrides Shelf in the Atlantic Ocean. They found that larger shells (i.e. mollusks) are immobile whereas ash can be transported a maximum of 10cm up or/and down a sedimentary column in deep ocean and shelf areas. Clough, et al. (1997) also presents 10cm of bioturbation mixing but for the Chuckchi shelf. As shown in Figure 9, Griggs, et al. (2015) has used X-ray microtomography to visualize post-depositional processes (e.g. bioturbation and sedimentary loading). The heterogeneity of sediment on cm-scale that Griggs, et al. (2015) present is consistent with heterogeneity of the grain size replicate samples from Figure 7. However, it is not applicable when trying to explain the 1.1m tephra curve in this study since the tephra in Figure 9 is transported <5cm vertically.

Third, Kaufman, et al. (2012) speculates about layers above the Aniakchak tephra being the result of landscape destabilization, i.e. downcutting by rivers exposing and transporting thick tephra layers and increased ice berg transport of sediment. This could possibly be an explanation for the diffuse and wide tephra signal in the sections investigated here from 2PC.

Aniakchak tephra age

Timing for the caldera-forming eruption of Aniakchak has been subject to some debate in the past decades. Riehle, et al. (1987) reported an age range between 2040 and 6400 BP based on radiocarbon dating. Miller and Smith (1987) used radiocarbon dating of burnt logs in pyroclastic flows to present 3430 ± 10 BP. A similar procedure was used by

Begét, et al. (1992) to present an age of 3430 ± 70 BP. Kaufman, et al.

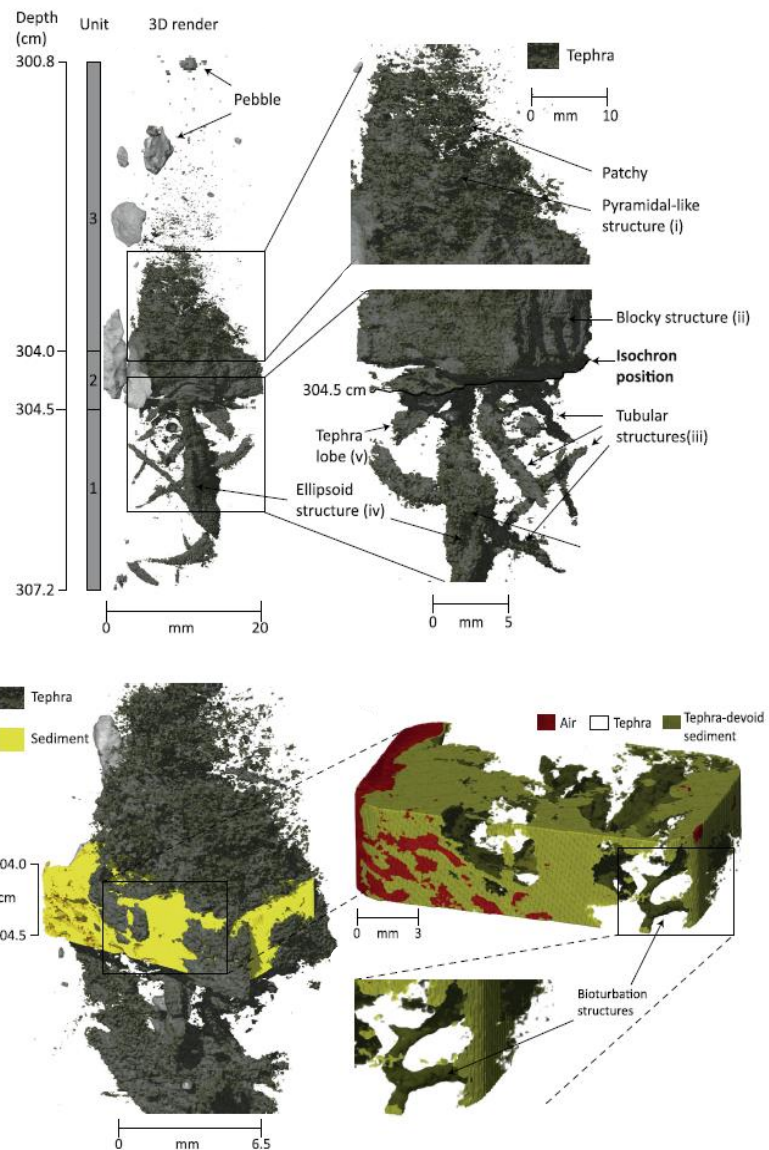


Figure 9. Modified from Griggs, et al. (2015). They illustrate the heterogeneity of a tephra deposit in marine sediment as caused by e.g. bioturbation.

(2012) and Blackford, et al. (2014) gives ages of 3700 ± 199 BP and 3491 ± 95 BP based on lake sediment cores. However, since the finding of tephra layers in Greenland ice cores, several studies have been done to identify and date those. By counting of the annual layers in the ice core, age uncertainty has been greatly reduced.

A tephra layer from the GRIP ice core was dated to 3595 ± 4 BP and identified as Minoan (Thera) in origin by Hammer, et al. (2003). This same layer was later re-interpreted by Pearce, et al. (2004) who argued that the geochemistry pointed towards Aniakchak. Abbott and Davies (2012) agreed with Pearce, et al. (2004) but recalculated the age of the tephra layer to 3591 ± 3 BP after correlation with other ice cores (GICC05 timescale).

Placing the isochron

As e.g. Griggs, et al. (2015) have demonstrated, placing an isochron in a marine core is no easy business.

The increase in tephra over *Increase X* shown as a saw tooth pattern in Figure 4 and 10 are here interpreted as Aniakchak, throughout based on geochemistry and high counts. Since bioturbation is limited to ≤ 10 cm as discussed above, this study interprets the cause of the wide signal as input lag, due to landscape denudation and secondary transport of reworked tephra. That would indicate an isochron at the lower part of the signal.

The isochron presented here has taken a ± 10 cm maximum of bioturbation into account, otherwise placing it at the very beginning of the signal (Figure 10). The isochron is here set to 704 ± 10 cm dbsf (Figure 10).

This has implications for the local reservoir age and hence the chronology of core 2PC. As shown in Figure 11, the new age model for 2PC suggests a ΔR of 482 years, which is almost 200 years more than first suggested.

Unfortunately, the 1cm samples from Figure 4 could not be used as an aid of finding the isochron. However, they proved useful in replicating the tephra peaks from the 5cm samples.

Despite low accuracy of the isochron, and despite ± 10 cm bioturbation, the

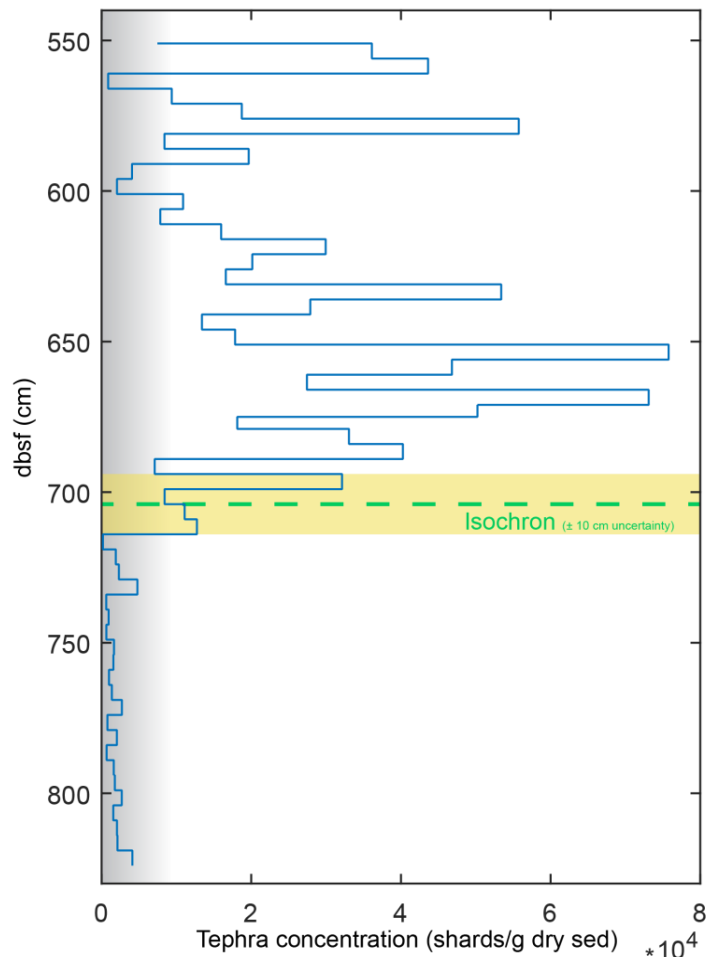


Figure 10. Isochron of the Aniakchak caldera-forming eruption as inferred from tephra counts, geochemistry and literature. The green dotted line indicates isochron and yellow field indicate the ± 10 cm of possible reworking. Grey field in left part of plot is the extent of interpreted background.

results are useful due to the high sedimentation rates at the site, where 2PC was retrieved. Although tiny in percentages, the distribution *does* show a correlation with peaks in tephra concentrations (Figures 7d and 7e). Rather than being a proxy for rhyolitic Aniakchak tephra - a lot of the $>127\mu\text{m}$ clasts are not rhyolitic, or tephra, and a great amount of the tephra is $<127\mu\text{m}$ - the peaks in $>127\mu\text{m}$ clasts could indicate an increase in the input of ice rafted detritus (IRD), or other transport mechanism leading to an increase in coarser clast fractions. That could be an important observation when explaining the $>1\text{m}$ spread of the tephra peak, seen in Figure 4, that is likely to have Aniakchak as origin. A possible complication regarding the grain size analysis could be that the small samples ($<0.5\text{g}$) risk of being unrepresentative for that depth. Griggs and Davies (2015) have used 3D imagery to visualize how heterogeneous core sediments can be, that is confirmed by the replicate samples taken at 649.5cm and 677.5cm (Figure 9).

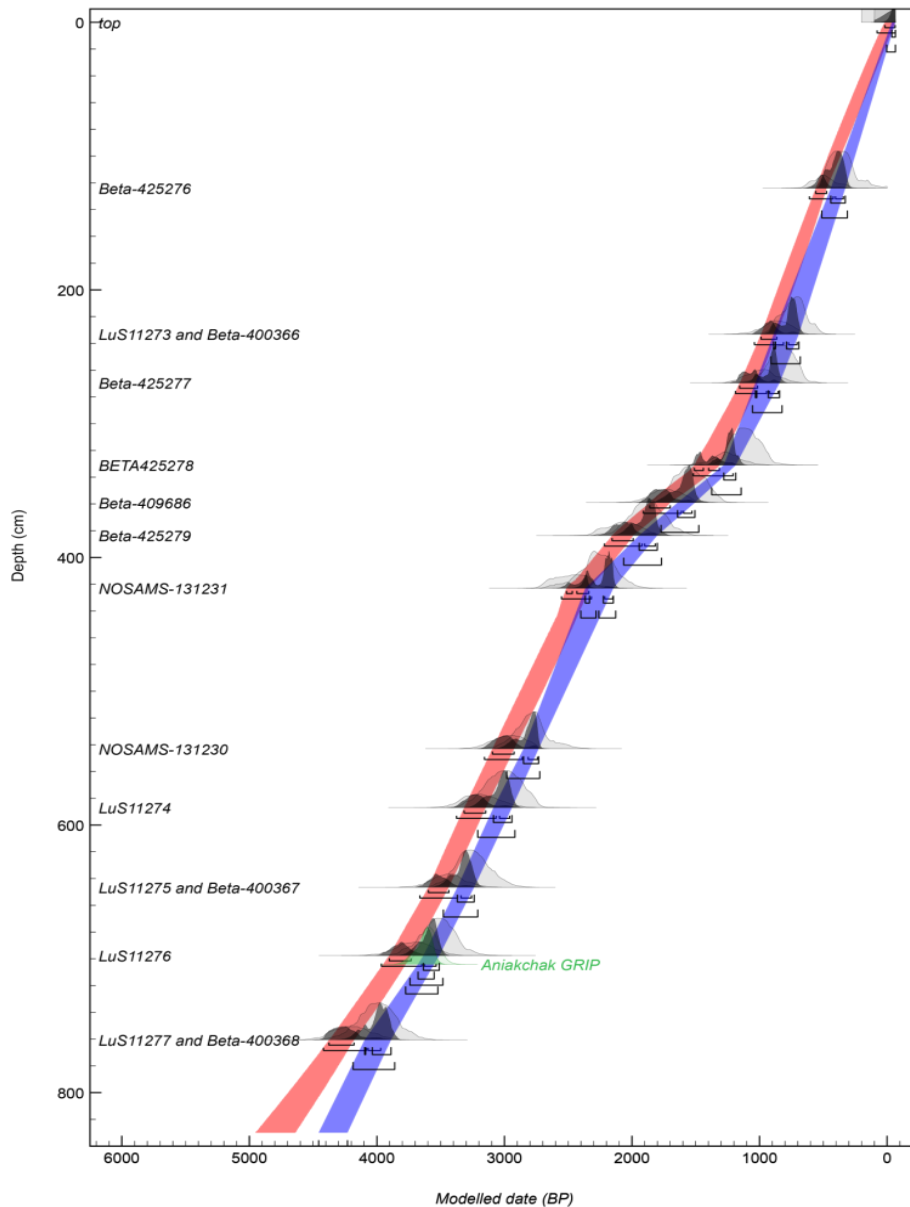


Figure 11. The previous (red) age model together with the new one (blue) for 2PC based on the ΔR derived from this study.

Conclusions

Clear rhyolitic tephra glass shards have been found throughout sampled sections (600-821cm dbsf in 2PC) repeatedly in this study. Variations in tephra counts indicate a saw tooth pattern surrounding a curve (interpreted as *Increase X*) at a depth where the Aniakchak II tephra is expected to have been deposited. This expectancy is based on 15 radiocarbon samples and a ΔR of 300 years which, in turn, is based on the ΔR in the Arctic Ocean. *Increase X* was subjected to high resolution samples of 1cm at the mid-point of this signal, reproducing the peaks, but did not further aid in the identification of an isochron. Instead, it is the 5cm samples that stand as main comparison when juxtaposing datasets. The tephra peaks overlying *Increase X* is interpreted as one or more different eruptions, possibly related to the 3.1ka tephra layer reported by Kaufman, et al. (2012).

All (30) tephra samples that were tested for geochemistry, and had an oxide count of >94%, showed a high level of resemblance with previous geochemical tests of Aniakchak tephra (e.g. Begét, et al. 1992; Blackford, et al. 2014). Although the sample spread wasn't optimal, it still corroborated the hypothesis that *Increase X* was one signal.

Results from the grain size analysis show a rather homogenous core, where mud of different sizes is dominating. Local heterogeneity's between different silt sizes and clay is shown by replicate samples at equal depth. This could possibly be explained by bioturbation and sediment loading structures (Clough, et al. 1997; Griggs, et al. 2015). If plotting >127 μ m grain size fractions, this data correlates to some degree with the peaks from *Increase X*, and the overlying tephra signals. The reproducibility of this data could use further study to see if grain size analysis can act as proxy for tephra.

If *Increase X* is indeed a result of the Aniakchak II eruption in 3591 ± 3 cal. yrs. BP (Abbott and Davies, 2014), then it is spread over too long a vertical distance to aid in determining the local ΔR , without introducing a more distinct isochron. This spread however is found to be too large to be explained by bioturbation, and therefore an isochron is proposed in this study to be placed at the lowest part of *Increase X*, where tephra counts first stand above the background levels. After correlation with the Aniakchak II eruption, this gives a ΔR of 482 years. Besides correcting the age model for core 2PC, this improved estimate of the local reservoir age could be of great significance to other studies in the Chukchi Sea of the late Holocene.

Acknowledgements

First and foremost Christof Pearce and Stefan Wastegård, for supervising this bachelor thesis project and for introducing me to the exciting world of tephrochronology. Thank you for your guidance and for making this project an enjoyable experience.

Carina Johansson at the Department of Geological Sciences for patient assistance during sampling and lab work, making sure of high quality results.

The crew of R/V Oden during the SWERUS (Leg 2) cruise in the summer of 2014. Without them, I wouldn't have a core to work on.

Emelie Modin and Jonas Fredriksson for proofreading.

References

- Abbott, P. M. & Davies, S. M., 2012. Volcanism and the Greenland ice-cores: the tephra record. *Earth-Science Reviews*, 115(3), pp. 173-191.
- Austin, W. E. N. et al., 1995. The ¹⁴C Age of the Icelandic Vedde ash: Implications for Younger Dryas Marine Reservoir Age Corrections. *Radiocarbon*, 37(1), pp. 53-62.
- Begét, J., Mason, O. & Anderson, P., 1992. Age, extent and climatic significance of the c. 3400 BP Aniakchak tephra, western Alaska, USA. *The Holocene*, 2(1), pp. 51-56.
- Blackford, J. J. et al., 2014. Age and impacts of the caldera-forming Aniakchak II eruption in western Alaska. *Quaternary Research*, 82(1), pp. 85-95.
- Boggs, Jr., S., 2011. *Principles of Sedimentology and Stratigraphy*. 5th ed. Upper Saddle River: Pearson Education, Inc..
- Clough, L. M. et al., 1997. Infaunal density, biomass and bioturbation in the sediments of the Arctic Ocean. *Deep-Sea Research II*, 44(8), pp. 1683-1704.
- Coulter, S. E. et al., 2012. Holocene tephras highlight complexity of volcanic signals in Greenland ice cores. *Journal of Geophysical Research*, 17(D21).
- Griggs, A. J. et al., 2015. Visualizing tephra deposits and sedimentary processes in the marine environment: The potential of X-ray microtomography. *Geochemistry, Geophysics, Geosystems*, 16(12), pp. 4329-4343.
- Hammer, C. U. et al., 2003. Thera eruption date 1645 BC confirmed by new ice core data?. In: M. Bietak, ed. *The Synchronisation of Civilisations in the Eastern Mediterranean..* Vienna: Austrian Academy of Science, pp. 87-94.
- Kaufman, D. S. et al., 2012. Late Quaternary tephrostratigraphy, Ahklun Mountains, SW Alaska. *Journal of Quaternary Science*, 27(4), pp. 344-359.
- Kylander, M. E., Lind, E. M., Wastegård, S. & Löwemark, L., 2011. Recommendations for using XRF core scanning as a tool in tephrochronology. *The Holocene*, 22(3), pp. 371-375.
- Lowe, D. J., 2011. Tephrochronology and its application: A review. *Quaternary Geochronology*, 6(2), pp. 107-153.

Miller, T. & Smith, R., 1987. Late Quaternary caldera-forming eruptions in the eastern Aleutian arc, Alaska. *Geology*, 15(5), pp. 434-438.

Pearce, N. J. G. et al., 2004. Identification of Aniakchak (Alaska) tephra in Greenland ice core challenges the 1645 BC date for Minoan eruption of Santorini. *Geochemistry, Geophysics, Geosystems*, 5(3).

Riehle, J. et al., 1987. The Aniakchak tephra deposit, a late Holocene marker horizon in western Alaska. *US Geological Survey Circular*, Volume 998, pp. 19-22.

Turney, C. S. M., 1998. Extraction of the rhyolitic component of Vedde microtephra from minerogenic lake sediments. *Journal of Paleolimnology*, 19(2), pp. 199-206.

Walker, M., 2005. *Quaternary Dating Methods*. 1st ed. Chichester: Wiley & Sons, Ltd..

Vinther, B. M. et al., 2006. A synchronised dating of three Greenland ice cores throughout the Holocene. *Journal of Geophysical Research*, 111(D13).